

RECOIL NUCLEI FROM THE DISINTEGRATION OF SILVER BY FAST PROTONS

N. I. BORISOVA, M. Ya. KUZNETSOVA, L. N. KURCHATOVA, V. N. MEKHEDOV, and L. V. CHISTYAKOV

Joint Institute for Nuclear Research

Submitted to JETP editor March 4, 1959

J. Exptl. Theoret. Phys. (U.S.S.R.) 37, 366-373 (August, 1959)

We have studied the angular and energy distributions of the recoil nuclei Ag^{106} , $\text{Ag}^{103,104}$, Nb^{90} , Zr^{89} , $\text{Rb}^{81,82}$ and Se^{73} produced when silver is bombarded by 480-Mev protons. These isotopes were separated from the reaction products radiochemically. The energy distribution of the recoil nuclei is shown to be exponential, and the parameters of the distribution are determined at an angle of 90° . We give a qualitative explanation of the observed distribution. The results confirm that Se^{73} , $\text{Rb}^{81,82}$, Zr^{89} , and Nb^{90} are formed by evaporation of α particles, protons, and neutrons.

INTRODUCTION

A number of recent papers¹⁻⁶ deal with recoil nuclei produced in reactions where high energy particles interact with complex nuclei. These papers give data on the kinetic energies of the reaction products, on their angular distributions, and on the excitation energy of the initial nucleus. The fundamental method used has been to determine an effective range in the target material for nuclei recoiling in the forward, backward, and perpendicular directions relative to the bombarding particles. Conclusions about the mechanisms of the reactions are made on the basis of the values obtained for these effective ranges. However, in our view there is a fundamental drawback to a study of the disintegration process through such experiments; that is, the effective range in the target material gives no information about the distribution of ranges of the recoil nuclei.

In the following we describe briefly some experiments to measure directly the ranges and angular distributions of some of the recoil nuclei from a thin silver target. The experiments were carried out in 1951-52, and are described in detail in reference 7. Particular attention was paid to reaction products appearing when many nucleons leave the initial nucleus. The statistical theory is, to some extent, suitable for describing the production of such reaction products, and, as will be shown below, these nuclei are formed by the evaporation of neutrons, protons and α particles. Our results on reaction products where only a few nucleons leave the initial nucleus (i.e., the radioactive isotopes of silver) are only preliminary.

METHOD

The problem reduced to determining the activity of a given isotope captured on a thin organic film placed near the silver target. Polystyrene was used to make the films. These were fitted into special containers, as shown in Fig. 1. The containers were made of very pure graphite and had thick walls (1 cm) to attenuate the protons bombarding the films. Container a was used to study the recoil nuclei at 90° , while container b was used to measure angular distributions. The target was a silver foil 0.5 mg/cm^2 thick. Spectral analysis of the foil showed admixtures of Mg, Si, Fe, Al, and traces of Pb ($< 10^{-3}\%$) and Au ($< 10^{-3}\%$).

The target was irradiated in the internal proton beam for an hour at a current of $\sim 0.1 \mu\text{a}$. After the bombardment, the reaction products of interest were extracted chemically from the films and the foil.

The following isotopes were studied: $\text{Ag}^{103} +$

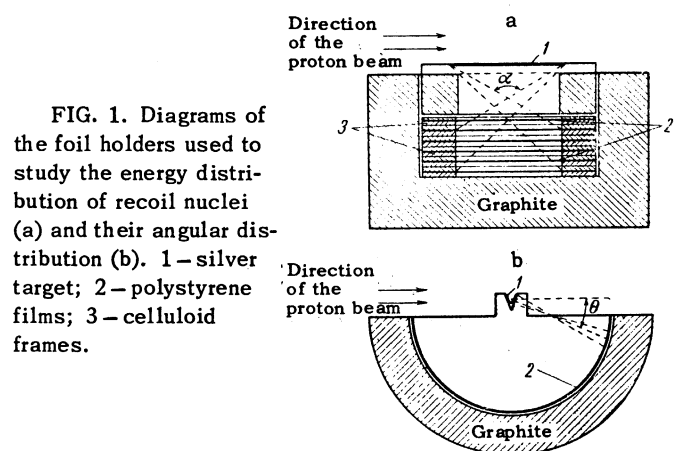


FIG. 1. Diagrams of the foil holders used to study the energy distribution of recoil nuclei (a) and their angular distribution (b). 1 - silver target; 2 - polystyrene films; 3 - celluloid frames.

Ag^{104} (β^+ , K), $T = 70$ min; Ag^{106} (K), $T = 8$ days; Zr^{89} (β^+ , K), $T = 80$ hrs; Nb^{90} (β^+ , K), $T = 16$ hrs; $\text{Rb}^{81} + \text{Rb}^{82}$ (β^+ , K), $T = 6$ hrs; and Se^{73} (β^+ , K), $T = 6.7$ hrs. Zr and Nb were not separated chemically. Zr^{89} and Nb^{90} could easily be distinguished by their decay curves.

In the chemical separation of these isotopes, the films were either burned in a muffle furnace and the ash then dissolved (the films having been first wrapped in filter paper), or dissolved in sulfuric acid with a suitable carrier. The latter was the method used with selenium. The chemical method used in the separation and purification was standard,⁸ except for minor details connected with the method for getting the active isotopes caught on the film into solution. The isotopes were identified by their half-lives. An electromagnet was used to determine the sign of the particle radiation. Half-lives measured in weak activities sometimes differed from accepted values (by not more than 20 or 25%).

The yield of an isotope was calculated with allowance for the time of irradiation, the length of time after cessation of the irradiation, the chemical yield, and corrections for the geometry of the experiment. The geometrical factors were necessary because the first and last films did not subtend the same solid angles α . The geometrical factors were calculated only roughly, assuming an isotropic angular distribution for the nuclei emitted. For the films on the ends, the correction factor for solid angle at the foil varied from 1.5 to 3.5.

Since the measurements were all relative, it was not necessary to introduce corrections for absorption of particle radiation in the counter walls, to take into account K capture, or to correct the results for self-absorption.

ANGULAR DISTRIBUTION OF THE REACTION PRODUCTS

For the recoil nuclei Ag^{106} , $\text{Ag}^{103,104}$, Nb^{90} , Zr^{89} , and $\text{Rb}^{81,82}$, the angular distributions were determined in three directions: forward, 90° to the proton beam, and backward. The target was a strip of foil 5 mm wide and bent into a semi-cylinder 40 mm long. Table I shows the angular

TABLE I

Isotope	Number of nuclei, %			
	Foil	forward ($5^\circ < \theta < 58^\circ$)	perpendicular ($63^\circ < \theta < 117^\circ$)	backward ($122^\circ < \theta < 175^\circ$)
Ag^{106}	90	6.0	2.0	2.0
$\text{Ag}^{103+104}$	90	6.0	3.0	1.0
Nb^{90}	70	21	7	2
Zr^{89}	66	24	7.5	2.5
Rb^{81+82}	≈ 30	≈ 40	≈ 20	≈ 5.0

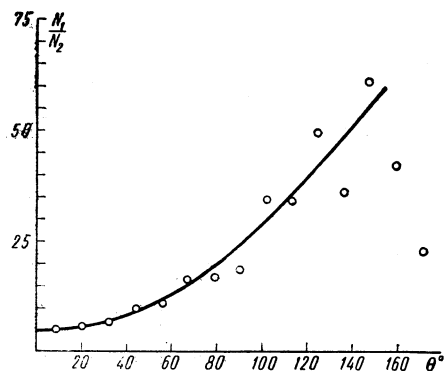


FIG. 2. Ratio of the activity in the first foil to that in the second as a function of the angle θ with the direction of the proton beam.

distribution obtained. The same table shows the intervals of angle θ covered at the three directions. The total measured activity associated with a given isotope (i.e., the number of nuclei emitted forward, backward and at 90° , plus half the activity remaining in the foil) was taken to be 100%. This sum, of course, underestimates the total number of nuclei (some intermediate parts of the film are discarded, some of the nuclei do not hit the detector after leaving the target, etc.). It was not possible to estimate the number of nuclei lost in these ways, and this reflected on the accuracy of the results. The accuracies of the data in Table I are not greater than 50%. The ratio of the number of nuclei emitted forward to those emitted backward is 2 or 3 times greater for all the products than it is for Ag^{106} .

We measured the kinetic energies of nuclei emitted at various angles θ to the proton beam. This was done by exposing two films in container b simultaneously and determining the ratio of the activities at the corresponding places. The first foil was 0.48 mg/cm^2 thick, while the second one had a thickness of 0.59 mg/cm^2 . The ratios of activities at corresponding places on the two foils are shown in Fig. 2. From the figure it is clear that nuclei emitted at small angles θ have relatively large kinetic energies.

A special experiment was carried out in another geometry to study the anisotropy of the emitted nuclei. In this experiment, a $1.7 \times 4 \text{ cm}$ strip of foil was oriented perpendicular to the proton beam. Aluminum collecting foils were fastened in special graphite holders on each side of the foil and parallel to it. These foils were 25μ thick and had an area 2.5 times greater than that of the radiator. The distances between the aluminum and silver foils were 2–3 mm; they were arranged to minimize the number of nuclei

TABLE II

Isotope	Observed activity, %			forward backward ratio	Yield* relative to Ag ^{103±104}	Relative thick-sample yield*
	forward	foil	backward			
Ag ¹⁰⁶	13.0	84.7	2.3	5.6	74.0	~70.0
Ag ¹⁰³⁺¹⁰⁴	17.0	81.0	2.0	8.5	100.0	100.0
Nb ⁹⁰	49.0	45.0	6.0	8.2	93.0	80.0
Zr ⁸⁹	49.0	46.0	5.0	8.7	42.0	38
Se ⁷³	67.0	21.0	12.0	5.6	1.5	~2

*The relative yields are calculated without reference to the absolute number of counts

missing the aluminum foils. In such a geometry, experimental errors were held to a minimum. The whole package was irradiated with protons having a mean energy 400 Mev. In this experiment, we looked for selenium rather than rubidium. The results are shown in Table II. For comparison, the table also gives the yields of the various nuclei studied in this experiment relative to yields found with thick silver samples.⁹

It is clear that the thick-target yields agree with those found here, to within 25%. As in the previous experiment, the fraction of nuclei emitted from the foil increases as the number of nucleons knocked out of the target nucleus increases. However, for Se⁷³, about 20% of the nuclei remain in the foil, i.e., their energies are insufficient to penetrate a layer of Ag 0.5 μ thick. It is difficult to make a definite conclusion about the dependence of the anisotropy on Z.

This experiment confirms that the forward/backward ratio for Ag¹⁰⁶ is less by a factor of almost two than it is for Ag¹⁰³⁺¹⁰⁴.

ENERGY DISTRIBUTION OF THE REACTION PRODUCTS

Using the geometry of Fig. 1a, the energy distribution of the recoil nuclei was studied for the same isotopes as those above, and also for Se⁷³ at an angle 90° ± 40°. For each element, the results of direct measurements of the fraction of nuclei having various ranges is shown in Fig. 3. The error bars shown are due to the thicknesses of the polystyrene films. The first point is half the activity remaining in the silver foil. As is evident from the figure, for each element the number of recoil nuclei decreases with increasing range. The range increases with decreasing Z of the product nucleus. In the region of small ranges and for light nuclei, the rate at which the curve drops decreases somewhat, the effect being more marked for smaller Z. In selenium, there is an irregularity in the distribution near a range 0.25 mg/cm². This irregularity is probably an experimental error and upon changing to an en-

ergy scale one can see that it is within the assigned limits of error. The largest range shown corresponds to an activity equal to or less than the counter background, i.e., 16 counts/min. Some indications of activities with longer ranges were found, but these are not shown on the graph because the counting rate was so slow the half life could not be determined. This made it difficult to find the longest range nuclei emitted.

The reaction products considered appear also as light fragments in the fission of uranium. This makes it possible to go from ranges to energies in our experiment by using the experimental range-energy curve for light uranium fission fragments.¹⁰ The curve used is shown in Fig. 4, which also shows the range-energy relation for fission fragments in silver.¹⁰ The curve for polystyrene was obtained using the atomic stopping power of polystyrene (the mean atomic number

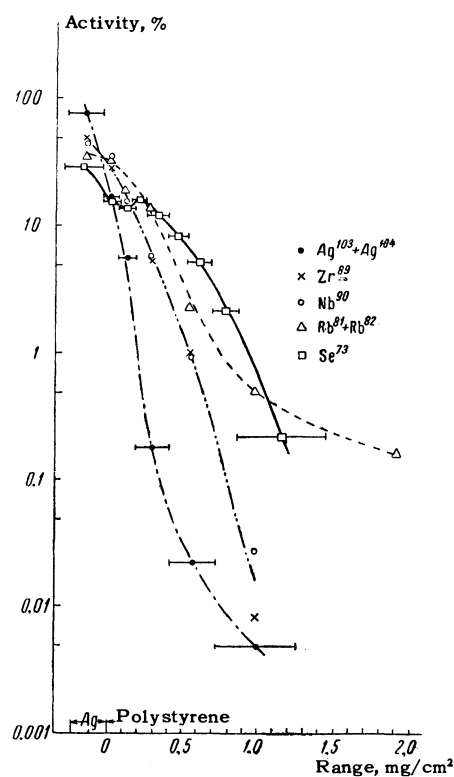


FIG. 3. Range distribution of nuclei recoiling at an angle 90° ± 40°.

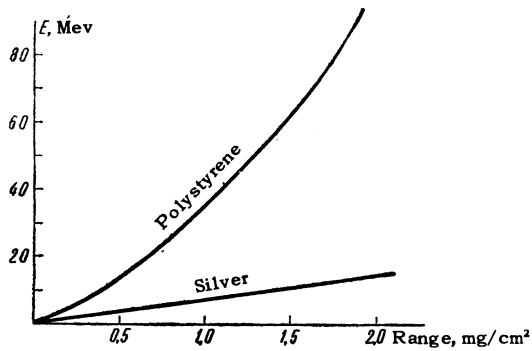


FIG. 4. Range-energy relation for the reaction products of interest.

being taken to be 3).

The masses of the isotopes studied differ from those of the light fission fragments of uranium by 7 to 10 units. This difference might lead to a slightly greater range (at a given energy) for the isotopes we are considering. However, this effect could not be taken into account and was neglected.

Figure 5 shows the energy distribution of the recoil nuclei. In going from ranges to energies, we also made corrections for geometrical factors. For all the curves, the first points correspond to half the activity remaining in the foil. They correspond to a range of 0.25 mg/cm² in silver, or an energy loss of 2.0 Mev. Although such a determination of the energy loss is somewhat artificial, the first points agree well with the remaining experimental points.

Figure 5 shows that, for all the reaction products, the number of nuclei decreases linearly with increasing logarithm of their energy. The slopes of the straight lines differ, the slope being steepest for silver and flattest for selenium.

DISCUSSION OF THE EXPERIMENTAL RESULTS

Energy can be imparted to a product nucleus either through a direct interaction, or after the formation of a compound nucleus. The energy and angular distributions of the recoil nuclei are obtained by combining the momenta obtained directly from the bombarding particle with the mean momentum possessed by the recoil nucleus after all particles have been emitted.

The momentum given a nucleus by the bombarding particle usually lies in the direction of motion of the protons, while the momentum transferred in evaporation has an isotropic distribution. The sum of these two momenta, one from direct interaction and one from evaporation, will be a minimum in the backward direction. Hence nuclei emitted backward must have less energy than

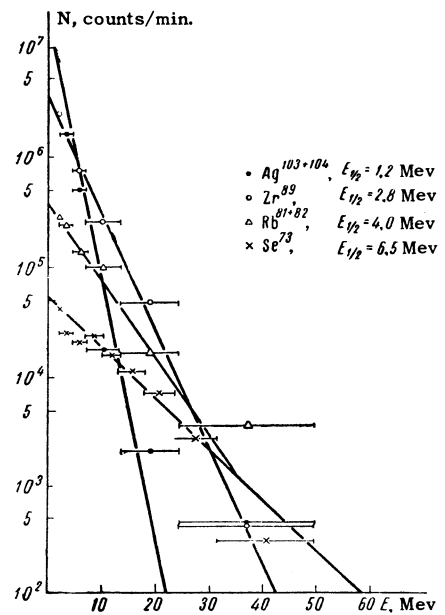


FIG. 5. Energy distribution of nuclei recoiling at an angle of $90^\circ \pm 40^\circ$.

those emitted at 90° or forward. This conclusion is supported by Fig. 2, which shows the ratio of activities in the first and second foils grows with increasing θ . From this it follows also that the energy distribution of the reaction products at 90° to the proton beam should be essentially determined by the mean energy transferred to the emitted particles. We note that in our case we can neglect cascade particles since they will have little effect on the distribution at 90° . Strictly speaking, one should take into account not only cascade processes, but also interactions where the momentum transferred by the bombarding particle does not lie in the direction of motion of the bombarding particle. The existence of high energy tails is presumably due to these two processes. The curve for $\text{Ag}^{103+104}$ in Fig. 5 shows that such events are rare, but do take place (about $1:10^4$). We neglect such details because of the computational difficulties involved.

Let us look at the average momentum a recoil nucleus has after all particles have evaporated. The problem of finding the mean momentum after a number of nucleons have been ejected independently and isotropically is analogous to the problem of finding the mean angle of multiple scattering when a fast particle traverses a layer of thickness d .^{*} In multiple scattering,^{11,12} the mean-square angle of scattering is given by

^{*}The method described below was proposed by B. T. Geĭlikman. We obtained similar results by considering the statistical equilibrium between the product nucleus and the emitted particles.⁷

TABLE III

Isotope	\bar{E} , Mev, experimental	\bar{E} , Mev, (n, p)	\bar{E} , Mev, (n, p, α)	Mean number of particles $\alpha : p : n$	Mean energy carried off			Total energy carried off (α , p, n)
					α	p	n	
Ag ¹⁰³⁺¹⁰⁴	2,6	0,4	0,4	0 : 0 : 4—5 (0 : 1 : 4—5)	—	—	—	—
Nb ⁹⁰	6	1,7	3,8	1,1 : 3,8 : 9,8	21	63	108	192 (200—210)
Zr ⁸⁹	6	1,9	4,1	1,3 : 4,4 : 9,4	24	73	103	200 (200—210)
Rb ⁸¹⁺⁸²	9	2,6	6,4	1,8 : 6,4 : : 12,4—13,4	33	106	136—147	275—286 (230—250)
Se ⁷⁸	14	4,3	9,7	2,5 : 9 : 16	46	148	176	370

$$\bar{\varphi}^2 = (\bar{\psi})^2 d/\lambda, \quad (1)$$

where λ is the mean free path, $(\bar{\psi})^2$ is the mean-square angle of scattering in one collision, and $d/\lambda = n$ is the number of collisions. In our case, this is the number of nucleons evaporated. The size of the angle corresponds to momentum.

Assuming, then, that when a definite kind of particle is emitted, the recoil nucleus gets a momentum of a certain fixed magnitude, the mean-square momentum of the recoil nucleus can be written

$$\sqrt{\bar{p}^2} = \bar{p}_{e1} \sqrt{n}. \quad (2)$$

The momentum distribution of the nuclei must be Gaussian, i.e.,

$$w(p^2) = w_0 e^{-\beta p^2}. \quad (3)$$

The constants β and w_0 are determined by normalization and evaluation of the mean, so that

$$\int_{-\infty}^{\infty} w(p^2) d\omega = 1, \quad \int_{-\infty}^{\infty} w(p^2) p^2 d\omega = \bar{p}^2, \quad (4)$$

where $d\omega = 4\pi p^2 dp$ is the volume element in momentum space. Finally, the momentum distribution can be written

$$w(p^2) = 0.165 (\bar{p}^2)^{-3/2} \exp \{-1.5 p^2 / \bar{p}^2\}. \quad (5)$$

Upon changing from momentum to energy, one can compare this distribution with the experimental one. The comparison was made in the following way. For each element in Fig. 5, we found the value $E_{1/2}$ at which the number of nuclei in the distribution decreased by a factor 2. From the value of $E_{1/2}$ we found the mean energy $\bar{E} = 1.5 E_{1/2} / 0.693$. On the other hand, \bar{E} can be obtained from the mean momentum $\bar{R} = \sqrt{p_{\alpha}^2} + \sqrt{p_p^2} + \sqrt{p_n^2}$ given a nucleus when it ejects a known number of particles. The calculation was made on the following assumptions: a) the nucleus evaporated only neutrons and protons (n, p); b) the nucleus evaporated alpha particles, neutrons, and protons (α , n, p). The mean energies carried away by alpha particles and protons, as obtained from ex-

periments with photoemulsions, are 14 and 8 Mev respectively.¹³⁻¹⁶ The numbers of alpha particles and protons were chosen to satisfy the relation* $\alpha/p = 0.3$;^{16,17} the mean energy of the evaporating neutrons was taken to be 2.5 Mev.¹⁸ The experimental and calculated quantities are shown in Table III.

The table shows that for four nuclei (Nb, Zr, Rb, and Se) the agreement between experimental and calculated values of \bar{E} is improved by taking into account the evaporation of α particles. Even in these cases, however, the calculated values of \bar{E} are 30 or 40% less than the experimental ones. The difference is presumably due to our neglect of cascade processes, though it is also possible that errors in the range-energy relation and approximation in the calculations played a role. Rough estimates show, for example, that if one were to assume that in the formation of Nb⁹⁰ there is emitted one cascade particle with an energy of ~ 30 Mev and travelling at 90° to the proton beam, then the discrepancy between the values of \bar{E} is decreased to almost one-half. Unfortunately, lack of experimental data precludes a more exact treatment of cascade processes. We propose to fill in this gap in subsequent work.

For Ag¹⁰³⁺¹⁰⁴ the value of \bar{E} calculated assuming that 4 to 6 nucleons evaporate is about 6 times smaller than the experimental one. Such a discrepancy can be removed only if we assume that each neutron emitted carries off an energy ~ 30 Mev. In this case most of the ejected neutrons must be formed in cascade processes, the observed radioactive silver isotope remaining after a sequence of knock-on events.

In spite of the limitations mentioned above, the energy spectrum of the recoil nuclei gives some information on the numbers of α particles, protons, and neutrons emitted and on their energies.

*The values of \bar{E} calculated under the assumptions $\alpha/p = 0.5$ and 0.4 differed but little from the value calculated with $\alpha/p = 0.3$.

One can then compute the excitation energy and what fractions of it are due to the various particles. In computing the excitation energy of the compound nucleus, one must take into account the binding energies of the particles ejected. The binding energy of an α particle was taken to be 4.5 Mev, while that of neutrons and protons was taken to be 8.5 Mev.¹⁹⁻²¹ The results of such calculations are shown in the last columns of Table III. The numbers in parentheses are the excitation energies calculated from the momentum given the compound nucleus by the incident proton.⁷ These excitation energies were obtained from the angular distributions of the corresponding reaction products, as shown in Table I. It is clear that the excitation energies agree satisfactorily with one another. The energy used to evaporate neutrons is almost one half of the total excitation energy.

We should like to express our sincere thanks to B. V. Kurchatov and to Prof. B. T. Geilikman for their help and valuable suggestions.

¹ Si-Chang Fung and I. Perlman, *Phys. Rev.* **87**, 623 (1952).

² R. E. Batzel and G. T. Seaborg, *Phys. Rev.* **82**, 607 (1951).

³ Sugarman, Campos, and Wielgoz, *Phys. Rev.* **101**, 388 (1956).

⁴ N. T. Porile, *Phys. Rev.* **108**, 1526 (1957).

⁵ F. P. Denisov and P. A. Cerenkov, *J. Exptl. Theoret. Phys. (U.S.S.R.)* **35**, 544 (1958); *Soviet Phys. JETP* **8**, 376 (1959).

⁶ L. V. Volkova and F. P. Denisov, *J. Exptl. Theoret. Phys. (U.S.S.R.)* **35**, 538 (1958); *Soviet Phys. JETP* **8**, 372 (1959).

⁷ V. N. Mekhedov, *Dissertation, Inst. Nuc. Prob. U.S.S.R. Acad. Sci.*, 1954.

⁸ Kurchatov, Mekhedov, Borisova, Kuznetsova, Kurchatova, and Chistyakov, *Сессия АН СССР по мирному использованию атомной энергии (Session of the Academy of Sciences of the USSR on the Peaceful Uses of Atomic Energy)*, 1955 [Engl. Transl. by U. S. Dept. of Commerce].

⁹ Kurchatov, Mekhedov, Kuznetsova and Kurchatova, *Сводный отчет ИЯП АН СССР (Summary Report of the Institute for Nuclear Problems Academy of Sciences, U.S.S.R.)* 1951.

¹⁰ C. B. Fulmer, *Phys. Rev.* **108**, 1113 (1957).

¹¹ B. Rossi and K. Greisen, *Interaction of Cosmic Rays with Matter* (Russ. Translation) IIL, 1950

¹² E. Fermi, *Nuclear Physics* (Russ. Translation) IIL, 1951.

¹³ Harding, Lattimore, and Perkins, *Proc. Roy. Soc. (London)* **196A**, 325 (1949).

¹⁴ N. Page, *Proc. Phys. Soc. (London)* **63A**, 250 (1950).

¹⁵ R. W. Deutsch, *Phys. Rev.* **92**, 515 (1953).

¹⁶ E. L. Grigor'ev and L. P. Solov'eva, *J. Exptl. Theoret. Phys. (U.S.S.R.)* **31**, 932 (1956); *Soviet Phys. JETP* **4**, 801 (1957).

¹⁷ P. E. Hodgson, *Phil. Mag.* **42**, 82 (1951).

¹⁸ Goldanski, Ignatenko, Mukhin, Pen'kina and Skoda-Ulyanov, *Phys. Rev.* **109**, 1762 (1958).

¹⁹ W. Heisenberg, *Vorträge über Kosmische Strahlung*, Berlin 1953.

²⁰ Y. Fujimoto and Y. Yamaguchi, *Progr. Theoret. Phys.* **5**, 787 (1950).

²¹ K. J. Le Couteur, *Proc. Phys. Soc.* **63A**, 498 (1950).

Translated by R. Krotkov